Draft version March 4, 2013
Preprint typeset using LaTeX style emulateapj v. 5/2/11

MASS-VARYING NEUTRINO COSMOLOGIES IN LIGHT OF CMB AND WEAK LENSING MEASUREMENTS

Giuseppe La Vacca[1,2] and David F. Mota[2]
[1]Physics Department "G. Occhialini", Milano-Bicocca University &
I.N.F.N., Sezione di Milano-Bicocca Piazza della Scienza 3, 20126 Milano, Italy and
[2]Institute of Theoretical Astrophysics, University of Oslo, 0315 Oslo, Norway

Draft version March 4, 2013

ABSTRACT

We study and constraint Mass-Varying Neutrino models using present and future available data. In these models, dark energy is a self-interacting scalar field directly coupled to neutrinos. We investigate two different potentials and both positive and negative coupling parameter β. This corresponds to increasing or decreasing neutrino mass, respectively. We explore couplings up to $|\beta| \lesssim 5$. In the case of the exponential potential, we find upper limits on $\omega_\nu < 0.004$ at 2-σ level. In the case of the inverse power law potential the null coupling can be excluded with more than 2-σ significance, the limits on the coupling being $\beta > 3$ for the increasing neutrino mass and $\beta < -1.5$ for the decreasing mass case. This is a clear sign of a preference for higer couplings. When including a prior on the neutrino mass today the upper limits on the coupling become $|\beta| < 3$ at 2-σ level for the exponential potential. Finally, we present Fisher forecast using the tomographic weak lensing from the Euclid-like experiment, also in combination with the CMB temperature and polarization spectra from the Planck-like mission. If considered alone, lensing data is very efficient in constraining ω_ν, giving a signal of a non-null neutrino mass with high significance. There is, however, a strong degeneracy in the β-ω_ν plane. When the two data sets are combined, the latter degeneracy remains, but the zero β value can be excluded at more than 2-σ.

1. INTRODUCTION

Present days astronomical observations strongly indicate there are two unknown components in the universe matter-energy budget. These are dark matter (DM) and dark energy (DE)(Riess et al. 1998; Perlmutter et al. 1999; Kowalski et al. 2008). The cosmological constant Λ is one of the simplest candidates for the nature of dark energy. Although so far consistent with all major observational probes (Wood-Vasey et al. 2007; Reid et al. 2010; Komatsu et al. 2011; Sullivan et al. 2011), it faces two major puzzles: 1) Why such a tiny value (the cosmological constant problem)? 2) Why Λ has become important only recently (the coincidence problem). Several possible solutions to these issues have been put forward. In particular, by identifying dark energy with a scalar field (Wetterich 1988; Peebles & Ratra 1988) and to couple it to either dark matter, or baryons or neutrinos (Wetterich 1995; Amendola 2000; Amendola et al. 2011; La Vacca et al. 2009; Kristiansen et al. 2010).

In this work, we study models where the dark energy field is coupled to neutrinos. These models are called Mass Varying Neutrino (MaVaN) quintessence (Fardon 2008; Keum 2007; Masiero 2005; Afshordi et al. 2005; Bi et al. 2005; Fardon et al. 2004; Bernardini & Bertolami 2009, 2008; de Holanda 2009; Spitzer 2006; Honda et al. 2006). Amendola et al. (2008a) have showed that the coincidence problem can indeed be solved for a mass growing neutrino with a coupling to quintessence somewhat larger than gravity.

Several authors have shown that important cosmological effects can appear within this class of models (Bjaelde et al. 2008; Brookfield et al. 2006b,a; Amendola et al. 2008b; Pettorino et al. 2009; Wetterich & Pettorino 2009; Pettorino 2009; Brouzakis et al. 2011; Nunes et al. 2011; Baldi et al. 2011a; Baldi 2011; Ayaita et al. 2011). Specially, when the neutrino mass is sufficiently big for neutrinos to be non-relativistic. When this happens, neutrinos feel the presence of the fifth force and can collapse into nonlinear structures, which are stable and bounded Wintergerst et al. (2010); Wetterich (2007); Bernardini & Bertolami (2009, 2008). It has been shown that these neutrino lumps form at redshift $z_{\rm nl} \approx 1-2$, when the neutrino fluctuations become nonlinear (Wetterich 2007; Mota et al. 2008; Wintergerst et al. 2010). These effects are mainly present in the strong coupling regime where a simple linear approach may be insufficient (Pettorino et al. 2010). Here we limit our analysis to the low coupling regime in which such instabilities are absent.

In this work we further investigate the cosmological signatures of MaVaN models and put constraints on them using the most updated observational data from the Cosmic Microwave Background (CMB) Radiation temperature anisotropies spectra, from the Large Scale Structure (LSS), and the Supernovae Type Ia (SNIa) luminosity distance. We start by investigating two different scalar field potentials and both positive and negative coupling parameter. This corresponds to increasing or decreasing neutrino mass, respectively. Finally, in the last section we present Fisher forecast using the tomographic weak lensing from an Euclid-like experiment (Laureijs et al. 2011), also in combination with the CMB temperature and polarization spectra from a Planck-like mission (The Planck Collaboration 2006).

2. THEORY

2.1. *The Cosmological Background Evolution*

MaVaN models involve a coupling between the DE scalar field and massive neutrinos. In a flat, homoge-

neous, Friedmann-Robertson-Walker universe with line-element

$$ds^2 = a^2(\tau)\left(-d\tau^2 + \delta_{ij}dx^i dx^j\right), \quad (1)$$

the Friedmann equation describes the universe expansion:

$$\mathcal{H}^2 \equiv \left(\frac{a'}{a}\right)^2 = \frac{a^2}{3}\sum_\alpha \rho_\alpha \ . \quad (2)$$

In this equation, $\rho_\alpha(\tau)$ is the energy density of the individual components α, including CDM, DE, neutrinos, baryons and radiation. The prime refers to the derivative with respect to conformal time τ.

The coupling of DE to the neutrinos results in the neutrino mass becoming a function of the scalar field, whose evolution is described by the coupling expression

$$\beta \equiv -\frac{d\ln m_\nu}{d\phi} \ . \quad (3)$$

We choose to take a constant β such that:

$$m_\nu \equiv \bar{m}_\nu e^{\beta\phi} \quad (4)$$

where $\bar{m}_\nu$ is a constant. An additional attractive force between neutrinos of strength $2\beta^2$ is mediated by the scalar field exchange. For $\beta \sim 1$ this corresponds to a strength comparable to gravity.

The existence of the coupling between DE and massive neutrinos can be formalized, assuming that the sum of the energy momentum tensors for the two species is conserved, but not the separate parts. We neglect a possible scalar field coupling to CDM, so that $\rho_c' = -3\mathcal{H}\rho_c$. This hypothesis requires DE and mass varying neutrinos obey the coupled conservation equations:

$$\rho_\phi' = -3\mathcal{H}(1+w_\phi)\rho_\phi + \beta\phi'(1-3w_\nu)\rho_\nu \quad (5)$$

$$\rho_\nu' = -3\mathcal{H}(1+w_\nu)\rho_\nu - \beta\phi'(1-3w_\nu)\rho_\nu \quad (6)$$

where, the energy density stored in the neutrinos is given by

$$\rho_\nu = \frac{1}{a^4}\int q^2 dq\, d\Omega\epsilon f_0(q), \quad (7)$$

and the pressure by

$$p_\nu = \frac{1}{3a^4}\int q^2 dq\, d\Omega f_0(q)\frac{q^2}{\epsilon}, \quad (8)$$

where $f_0(q)$ is the usual unperturbed background neutrino Fermi-Dirac distribution function

$$f_0(\epsilon) = \frac{g_s}{h_P^3}\frac{1}{e^{\epsilon/k_B T_0}+1}, \quad (9)$$

and $\epsilon^2 = q^2 + m_\nu^2(\phi)a^2$ (q denotes the comoving momentum). As usual, g_s, h_P and k_B stand for the number of spin degrees of freedom, Planck's constant and Boltzmann's constant respectively. In the following we will assume that the neutrinos decouple whilst they are still relativistic, and therefore the phase-space density only depends upon the comoving momentum.

The energy density and pressure of the quintessence field are given by

$$\rho_\phi = \frac{\phi'^2}{2a^2} + V(\phi), \quad p_\phi = \frac{\phi'^2}{2a^2} - V(\phi), \quad w_\phi = \frac{p_\phi}{\rho_\phi} \ . \quad (10)$$

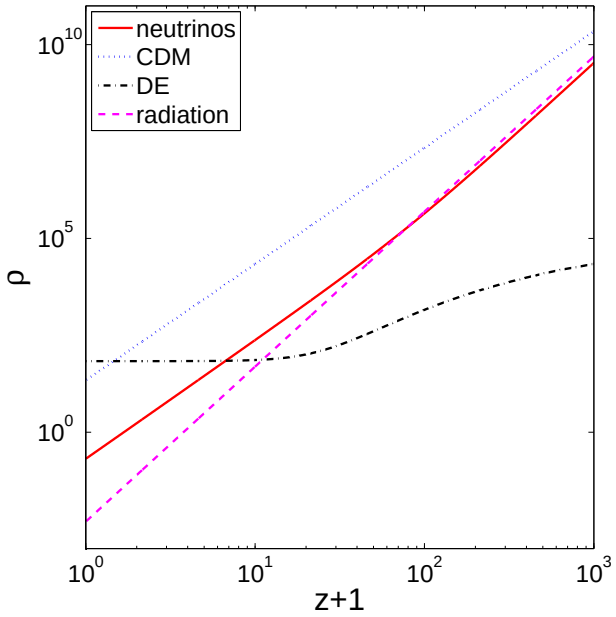

FIG. 1.— Energy density evolution of different components, as specified in the legend, for the potential (12), with $\beta = -1.9$, $\alpha = 0.021$, $\omega_\nu = 0.0010$, $\omega_{CDM} = 0.1097$, $\omega_b = 0.0224$, $h_0 = 70$.

Taking into account the energy conservation of the coupled neutrino-dark energy system, one can immediately find that the evolution of the scalar field is described by a modified Klein-Gordon equation:

$$\phi'' + 2\mathcal{H}\phi' + a^2\frac{dV}{d\phi} = a^2\beta(\rho_\nu - 3p_\nu) \ . \quad (11)$$

This equation contains an extra source term with respect to the uncoupled case, which accounts for the energy exchange between the neutrinos and the scalar field.

Here we investigate two different expressions for the DE potential: an exponential potential (Wetterich 1988; Ferreira & Joyce 1998):

$$V(\phi) \propto e^{-\alpha\phi} \quad (12)$$

and an inverse power-law (Steinhardt et al. 1999; Binetruy 1999)

$$V(\phi) \propto (M/\phi)^2 \ . \quad (13)$$

Both α in (12) and M in (13) are constant. In particular α is a free parameter which determines the slope of the potential and thus the DE fraction at early times. On the other hand, M defines the potential energy scale and, together with $\bar{m}_\nu$ in Eq. 4, is used to set the convergence of the model to the actual cosmology.

Once the potential (12) or (13) is given, the evolution equations can be numerically solved. In the very early universe, neutrinos are still relativistic and almost massless, with $p_\nu = \rho_\nu/3$ and the coupling term in eqs.(5), (6), (11) vanishes.

However, as soon as neutrinos become nonrelativistic, the coupling term $\sim \beta\rho_\nu$ becomes significantly different from zero, affecting also the evolution of the field ϕ. As shown in Fig. 1, ρ_ν and ρ_ϕ change behavior for $z < 6$: the value of the scalar field stays 'almost' constant and the frozen scalar field potential mimics a cosmological constant. According to this model, at the present time

neutrinos are still subdominant with respect to CDM, though in the future they will take the lead. For our choice of the parameters neutrino pressure terms may be safely neglected for redshifts $z_{nr} < 4$; before that redshift neutrinos free stream as usual relativistic particles.

2.2. *Perturbed Equations*

In order to compute the evolution of cosmological perturbations in our model. we work in the synchronous gauge, taking the line element to be

$$ds^2 = -a^2 d\tau^2 + a^2 \left(\delta_{ij} + h_{ij}\right) dx^i dx^j. \tag{14}$$

the perturbed Klein-Gordon equation is given by (Brookfield et al. 2006b):

$$\ddot{\delta\phi} + 2H\dot{\delta\phi} + \left(k^2 + a^2 \frac{d^2V}{d\phi^2}\right)\delta\phi + \frac{1}{2}\dot{h}\dot{\phi} = \tag{15}$$
$$-a^2\left[\frac{d\ln m_\nu}{d\phi}(\delta\rho_\nu - 3\delta p_\nu) + \frac{d^2\ln m_\nu}{d\phi^2}\delta\phi(\rho_\nu - 3p_\nu)\right].$$

For the neutrinos we use the perturbed part of the energy momentum conservation equation for the coupled neutrinos

$$T^{\mu}{}_{\gamma;\mu} = \frac{d\ln m_\nu}{d\phi}\phi_{,\gamma} T^{\alpha}_{\alpha} \tag{16}$$

to calculate the evolution equations for the neutrino perturbations (T^{α}_{α} stands for the trace of the neutrino energy momentum tensor). Taking $\gamma = 0$ we derive the equation governing the evolution of the neutrino density contrast , $\delta_\nu \equiv \frac{\delta\rho_\nu}{\rho_\nu}$ whilst taking $\gamma = i$ (spatial index) yields the velocity perturbation equation $\theta_\nu \equiv ik_i v^i_\nu$, with the coordinate velocity $v^i_\nu \equiv dx^i/d\tau$:

$$\dot{\delta}_\nu = 3\left(H + \beta\dot{\phi}\right)\left(w_\nu - \frac{\delta p_\nu}{\delta\rho_\nu}\right)\delta_\nu - (1+w_\nu)\left(\theta_\nu + \frac{\dot{h}}{2}\right)$$
$$+\beta\left(1-3w_\nu\right)\dot{\delta\phi} + \frac{d\beta}{d\phi}\dot{\phi}\delta\phi\left(1-3w_\nu\right), \tag{17}$$

$$\dot{\theta_\nu} = -H(1-3w_\nu)\theta_\nu - \frac{\dot{w_\nu}}{1+w_\nu}\theta_\nu + \frac{\delta p_\nu/\delta\rho_\nu}{1+w_\nu}k^2\delta_\nu$$
$$+\beta\frac{1-3w_\nu}{1+w_\nu}k^2\delta\phi - \beta(1-3w_\nu)\dot{\phi}\theta_\nu - k^2\sigma_\nu. \tag{18}$$

The variable σ_ν represents the neutrino anisotropic stress. It is the presence of the additional coupling terms in these expressions for the growth of the neutrino density and velocity perturbations, as well as the modifications to the evolution of the cosmological background, which alters the behaviour of the neutrino perturbations in comparison with the standard uncoupled case.

3. METHODS AND DATA

Two are the methods we use to test MaVaN theory against cosmological data: the likelihood analysis through Markov-Chain Monte-Carlo (MCMC) technique and the Fisher information matrix.

The CMB temperature and polarization anisotropy spectrum and matter power spectrum are calculated by suitably modifying CAMB (Lewis et al. 2000) to contemplate MaVaN's equations as described above. To ensure the accuracy of our calculations, we directly integrate the neutrino distribution function, rather than using the standard velocity weighted series approximation scheme.

For the MCMC analysis, we use a modified version of the publicly available code CosmoMC (Lewis & Bridle 2002) to explore the parameter space. We consider the following basic set of parameters:

$$\{\omega_b, \omega_{CDM}, H_0, z_{re}, \mathrm{n_s}, \ln \mathrm{A_s}, \omega_\nu, \beta\},$$

plus α when the exponential potential is involved. Here: $\omega_{b,CDM,\nu}$ are the physical baryon, total dark matter and neutrino density parameters, $\omega_{b,CDM,\nu} = \Omega_{b,CDM,\nu}h^2$, where h is the dimensionless Hubble parameter H_0; z_{re} is the redshift of reionization; n_s is the scalar spectral index; A_s denotes the amplitude of the scalar fluctuations at a scale of $k = 0.05$ Mpc^{-1}. The sum of ν masses is directly related to the neutrino density parameter through the relation $M_\nu = \Sigma m_\nu = \omega_\nu \cdot 93.5$ eV, assuming 3 equal mass ν's.

All parameters are given flat priors, unless otherwise stated explicitly. We choose to span only the low coupling regime up to $|\beta| < 5$, since linear perturbations become unstable for high couplings, *e.g.* $|\beta| \sim 50$. This is not a new issue in MaVaNs models, where many other authors have reported those instabilities (Mota et al. 2008; Wintergerst et al. 2010; Afshordi et al. 2005; Franca et al. 2009). However, there are several other claims in the literature that as the neutrino perturbations become nonlinear, those structure virialise and become stable (Pettorino et al. 2010; Baldi et al. 2011b). Hence, the strongly coupled mass-varying neutrino models may not be ruled out by the large scale structure formation in the linear regime, such as the integrated Sachs-Wolfe effect or the matter power spectra. In spite of the many attempts to understand and manage those "non-linearities" (Pettorino et al. 2010; Baldi et al. 2011b), a proper method of coping with these effects in a MCMC method to probe the parameter space of the models in the high β regime is still lacking. Therefore, we leave the strong coupling regime for a future work. In our MCMC analysis we assume that the Universe is spatially flat.

With the aim of obtaining the best estimate of the cosmological parameters, we combine different CMB datasets with data from large scale structure and SNIa. In particular, for the CMB temperature anisotropy spectra we considered the 7 year data from the WMAP satellite (WMAP7, see *e.g.* Komatsu et al. (2011)), plus higher multipole data from CBI (Sievers et al. 2007), ACBAR (Reichardt et al. 2009), VSA (Dickinson et al. 2004) experiments. For the matter power spectrum we choose the results from the SDSS survey (Tegmark et al. 2006). Constraints on the recent expansion history of the Universe are given by the SNIa observations from the Union2 compilation (Amanullah et al. 2010). We also apply additional priors on the Hubble parameter $H_0 = 74.2 \pm 3.6$ (Riess et al. 2009).

In addition to the likelihood analysis, we tested the power of future CMB and weak lensing data in constraining MaVaN's parameters using the Fisher formalism (Fisher 1935; Tegmark et al. 1997).

Fisher information measures the amount of information that observable random variables $\mathbf{X} = (\mathbf{X}_1, \ldots \mathbf{X}_n)$

provide about unknown parameters $\boldsymbol{\theta} = (\theta_1, \dots \theta_k)$ upon which the probability of $\mathbf{X}$ depends. Let $\mathcal{L}(\mathbf{X}|\boldsymbol{\theta})$ denote the likelihood function, yielding the probability that a model defined by the parameters $\boldsymbol{\theta}$, gives the set of observables $\mathbf{X}$. In our case $\mathbf{X}_\alpha$ are CMB anisotropy and weak lensing spectra. Then the Fisher information matrix is given by the $k \times k$ symmetric matrix:

$$\mathbf{F}_{ij}(\boldsymbol{\theta}) = \left\langle -\frac{\partial^2 \log \mathcal{L}(\mathbf{X}|\boldsymbol{\theta})}{\partial\theta_i \partial\theta_j} \right\rangle \ , \tag{19}$$

the average $\langle \dots \rangle = \int \mathcal{L}(\mathbf{X}|\boldsymbol{\theta}) \dots d^n\mathbf{X}$ is taken over all possible data realizations, given the model parameters. One useful property of the Fisher information matrix is the Cramér-Rao theorem. It states that the variance for the parameter θ_i about any unbiased estimator value cannot be inferior to $(\mathbf{F}^{-1})_{ii}^{1/2}$, if the other parameters are estimated from the data as well and marginalized, or $(\mathbf{F}_{ii})^{-1/2}$, if all the other parameters are known. Moreover, the information is additive, so that the total information allowed by two independent experiments is the sum of the information from each experiment separately.

It is worth noting that the likelihood can be locally approximated by a multivariate Gaussian distribution, Taylor expanding to second order (the first non-vanishing term, up to an irrelevant additive constant) around its maximum $\hat{\boldsymbol{\theta}}$ which, in the limit of large data sets, becomes the best unbiased estimator of the actual parameter set. Then the likelihood becomes:

$$\mathcal{L}(\mathbf{X}|\boldsymbol{\theta}) \propto \tag{20}$$
$$\exp\left[-\frac{1}{2}(\mathbf{X_{obs}} - \mathbf{X}(\boldsymbol{\theta}))^T \mathbf{C}(\boldsymbol{\theta})^{-1} (\mathbf{X_{obs}} - \mathbf{X}(\boldsymbol{\theta}))\right]$$

where $\mathbf{X_{obs}}$ and $\mathbf{X}(\boldsymbol{\theta})$ are respectively the observed and the theoretical values of the observables $\mathbf{X}$ and

$$\mathbf{C}_{ij}(\boldsymbol{\theta}) = \left[\left. \frac{\partial^2 \mathcal{L}(\mathbf{X}|\boldsymbol{\theta})}{\partial\theta_i \partial\theta_j} \right|_{\boldsymbol{\theta}=\hat{\boldsymbol{\theta}}} \right]^{-1} \tag{21}$$

is a positive semi-definite non-singular matrix, dubbed *covariance matrix* of the θ_i.

Therefore, under the hypothesis of a gaussian likelihood, the Fisher information matrix components are the expectation values of $\mathbf{C}^{-1}(\hat{\boldsymbol{\theta}})$. Accordingly, the inverse of the Fisher matrix is an estimate of the covariance matrix of the parameters $\mathbf{C}(\boldsymbol{\theta}) \approx \mathbf{F}^{-1}$. This shows that the Fisher matrix analysis represents only an approximation to the true likelihood and its results could significantly vary from the MCMC ones, especially if the parameters do have not a gaussian distribution.

It can be shown (Tegmark et al. 1997) that, when the probability distribution is gaussian, the fisher information matrix (19) reduces to

$$\mathbf{F}_{ij}(\boldsymbol{\theta}) = \frac{1}{2}\mathrm{Tr}\left[\mathbf{C^{-1}C}_{,i}\,\mathbf{C^{-1}C}_{,j}\right] \ , \tag{22}$$

if the means of the data are fixed.

4. MCMC RESULTS

4.1. *Cosmological data*

In the case of the exponential potential (12), likelihood contours and distributions for increasing ($\beta > 0$) or decreasing ($\beta < 0$) ν mass are shown in Fig. 2. We report plots for ω_ν, α and β which are the most significant parameters in our models, the constraints on the other parameters not considerably differing from the ΛCDM case.

For both increasing and decreasing mass, no stringent constraints can be put on the coupling β, whose upper limit exceeds $|\beta| = 5$ yet at 68% confidence level (CL). On the contrary, the ν density parameter is well constrained at 95% CL: $\omega_\nu < 0.0034$ (decreasing mass) and $\omega_\nu < 0.0032$ (increasing mass). This limits are ~ 3 times narrower than those found in Brookfield et al. (2006b). In term of today neutrino mass these values attest an upper limit to $m_\nu \simeq 0.32$eV. The limits on α are centered around zero in both cases: $-1.12 < \alpha < 0.77$ (decreasing mass) and $-0.89 < \alpha < 1.05$ (increasing mass) at 1-σ.

Let us underline that the results show a common behaviour in the β *vs.* ω_ν plots, almost symmetric with respect to the sign of β. In fact a degeneracy appears between the two parameters so that high $|\beta|$ are in agreement with low neutrino content, or equivalently low neutrino mass.

In Fig. 3 we reported likelihood contours for the case of the inverse power-law potential as in (13). This potential type was not previously considered in Brookfield et al. (2006b). In the β *vs.* ω_ν plots the zero coupling is apparently excluded with statistical significance higher than 95% confidence level (CL), with $\beta > 3$ for the increasing neutrino mass and $\beta < -1.5$ for the decreasing mass case at 2-σ. In particular, the growing neutrino mass case exhibits an explicit preference for high β values, in agreement with Amendola et al. (2008a). For ω_ν only upper limits can be found at 95% CL: $\omega_\nu < 0.0017$ (decreasing mass) and $\omega_\nu < 0.0423$ (increasing mass).

4.2. *External priors*

Complementary information to cosmological data can be obtained by taking into account priors on parameters coming from external measurements. In such a way a better knowledge of the other parameters can be obtained.

In our analysis we fix the value of the neutrino mass today (and as a consequence ω_ν), using two possible options, $m_\nu = 0.2$ eV and $m_\nu = 0.3$ eV . These values are within the range of the claimed ν_e mass detection in the Heidelberg-Moscow experiment (Klapdor-Kleingrothaus et al. 2004; Klapdor-Kleingrothaus 2005). Also the KATRIN experiment (Sturm 2011) is expected to constraint the value of the neutrino mass with a sensitivity in the sub-eV range.

Beside fixing ω_ν, we chose to fix the baryon density parameter $\Omega_b h^2 = 0.022$, as constraints on this parameter are not significantly modified by neutrino-DE coupling. Also the value for $H_0 = 72$ km s^{-1}Mpc^{-1} is kept constant.

In the exponential potential case we are therefore left with a cosmological model requiring six parameters: β, α, $\Omega_{CDM}h^2$, z_{re}, A_s and n_s.

In Fig. 4 and 5 we show likelihood contours and distributions for increasing and decreasing neutrino mass, respectively. The most significant result in both cases is the improvement in parameter constraints. In fact the limits on the coupling become more stringent, with an upper value $|\beta| \simeq 2 \div 3$, and the distributions for α be-

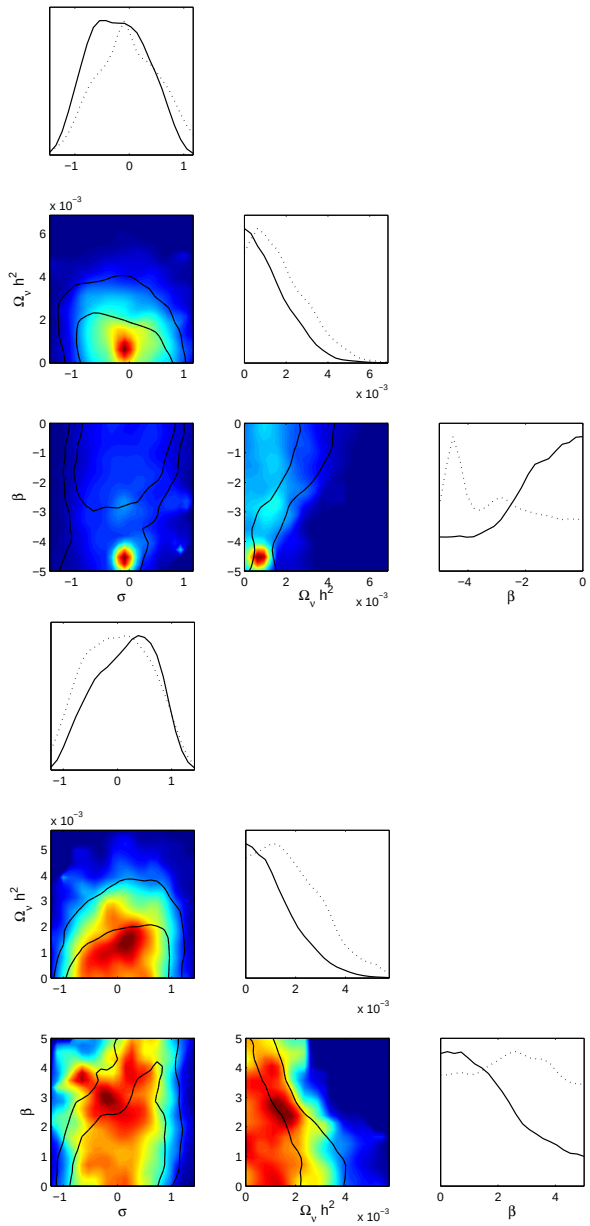

FIG. 2.— In the upper (lower) panel, likelihood contours and distributions are shown for decreasing (increasing) neutrino mass in the exponential potential case. For the plots on the diagonal, dotted lines are mean likelihoods of samples, solid lines are marginalized probabilities. Similarly, for the coloured plots, black lines are 1- and 2-σ contours of the marginalized probability distribution, while the colours refer to mean likelihood degradation from the top (dark red) to lower values.

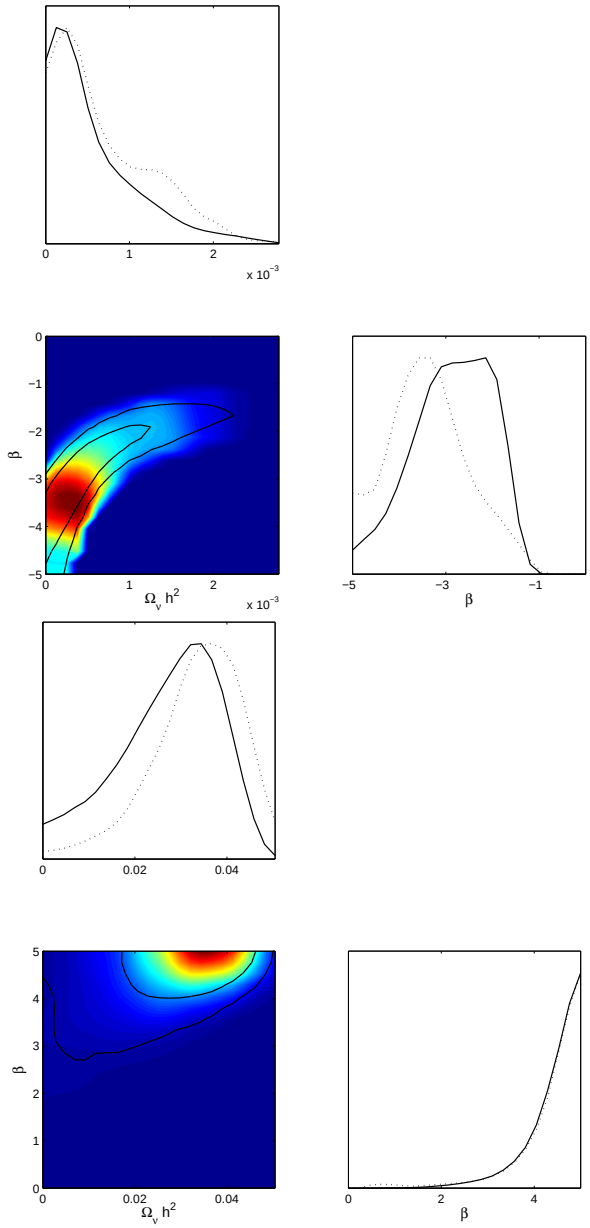

FIG. 3.— As in Fig. 2, when the power-law potential is considerd.

come narrower, but always compatible with zero at 68% CL.

It is worth to notice that the colored plot in the upper panel in Fig. 4 shows a complex structure for the likelihood contours in which the upper value of the coupling still exceeds $\beta = 5$. This effect can be mainly ascribed to the peculiar features of the likelihood in Fig. 2 which are completely lost when considering a prior with higher mass.

5. FISHER MATRIX FORECASTS

In the next few years new and more accurate datasets will be available. In this section we show Fisher matrix analysis results from the combination of the CMB anisotropies and the tomographic weak lensing (TWL) spectra.

We considered the case of the exponential potential with an exponential coupling. The fiducial parameters θ_α are shown in Tab. 1. This two sets correspond to the maximum area of the likelihood as determined in par. 4.1 and are chosen to be exactly the same, with the only exception of the sign of β.

The Fisher matrix for CMB power spectrum is given by (Zaldarriaga & Seljak 1997; Zaldarriaga et al. 1997; Rassat et al. 2008):

$$F^{\rm CMB}_{\alpha\beta} = \sum_l \sum_{X,Y} \frac{\partial C_{X,l}}{\partial \theta_\alpha} {\rm COV}^{-1}_{XY} \frac{\partial C_{Y,l}}{\partial \theta_\beta} \qquad (23)$$

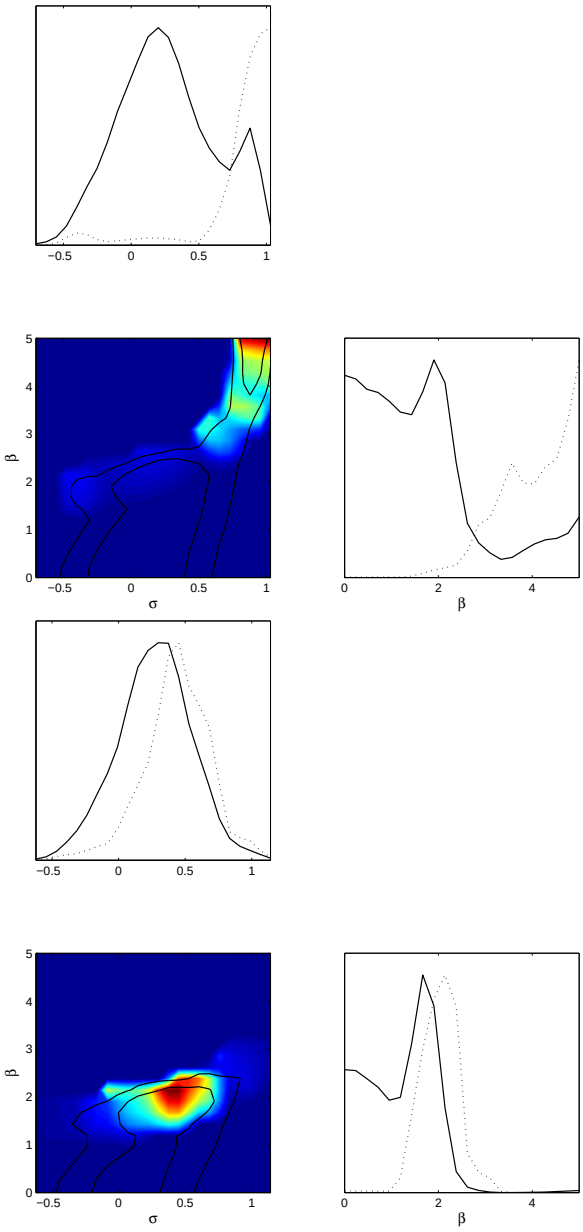

FIG. 4.— Upper (lower) panel shows posterior constraints for the exponential potential with increasing ν mass. Here we fixed $m_\nu = 0.2$eV ($m_\nu = 0.3$eV), $\omega_b = 0.022$, $\mathrm{H}_0 = 72$

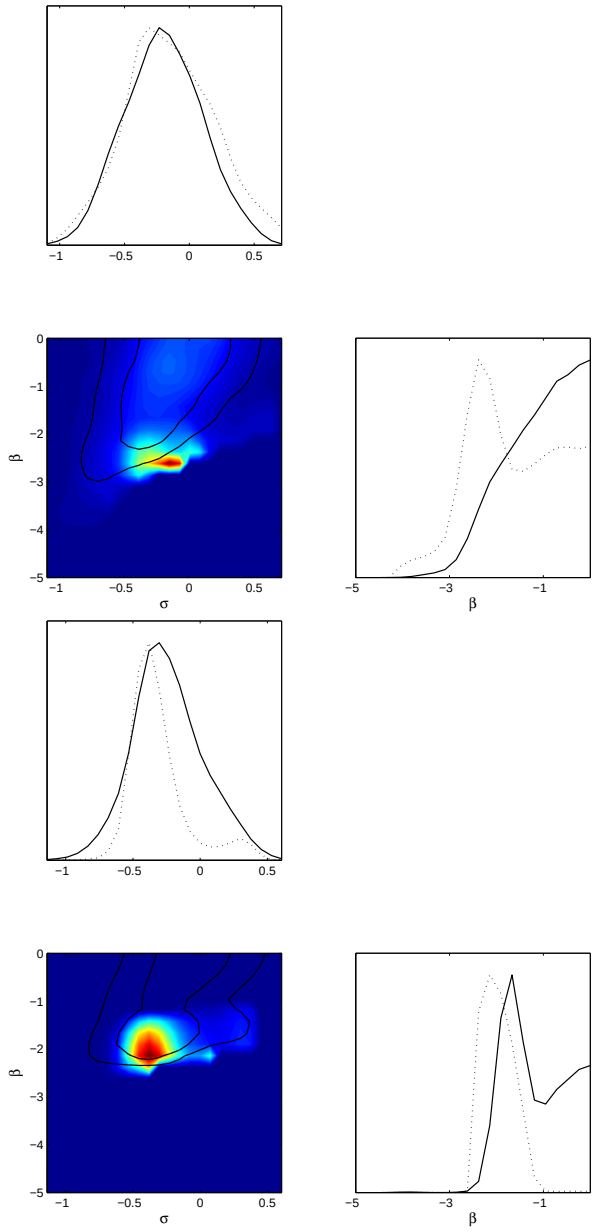

FIG. 5.— Upper (lower) panel shows posterior constraints for the exponential potential with decreasing ν mass. Here we fixed $m_\nu = 0.2$eV ($m_\nu = 0.3$eV), $\omega_b = 0.022$, $\mathrm{H}_0 = 72$

TABLE 1
FIDUCIAL COSMOLOGICAL PARAMETERS FOR THE EXPONENTIAL POTENTIAL, CONSISTENT WITH FIG. 2.

Parameter	ω_b	ω_{CDM}	H_0	z_{re}	$\mathrm{n_s}$	$\ln \mathrm{A_s}$
Value	0.0224	0.1097	69	11	0.95	2.09×10^{-9}
Parameter	ω_ν	α	β			
Value	0.0010	0.02	±1.9			

where $C_{X,l}$ is the harmonic power spectrum for the temperature–temperature ($X \equiv TT$), temperature–E-polarization ($X \equiv TE$) and the E-polarization–E-polarization ($X \equiv EE$) power spectrum. Under the assumption of a Gaussian likelihood distribution, the covariance COV^{-1}_{XY} of the errors of the various power spectra is given in terms of $C_{X,l}$ with

$$\mathrm{COV}_{T,T} = f_l \left(C_{T,l} + W_T^{-1} B_l^{-2}\right)^2 \quad (24)$$

$$\mathrm{COV}_{E,E} = f_l \left(C_{E,l} + W_P^{-1} B_l^{-2}\right)^2 \quad (25)$$

$$\mathrm{COV}_{TE,TE} = f_l \Big[C_{TE,l}^2 + \left(C_{T,l} + W_T^{-1} B_l^{-2}\right)\left(C_{E,l} + W_P^{-1} B_l^{-2}\right) \Big] \quad (26)$$

$$\mathrm{COV}_{T,E} = f_l C_{TE,l}^2 \quad (27)$$

$$\mathrm{COV}_{T,TE} = f_l C_{TE,l} \left(C_{T,l} + W_T^{-1} B_l^{-2}\right) \quad (28)$$

$$\mathrm{COV}_{E,TE} = f_l C_{TE,l} \left(C_{E,l} + W_P^{-1} B_l^{-2}\right) \ , \quad (29)$$

where $f_l = \frac{l}{(2l+1)f_{\rm sky}}$ and $W_{T,P} = (\sigma_{T,P}\theta_{\rm fwhm})^{-2}$ is the weight per solid angle for temperature and polarization, with a 1-σ sensitivity per pixel of $\sigma_{T,P}$ with a beam of $\theta_{\rm fwhm}$ extend. The beam window function is given in terms of the full width half maximum (fwhm) beam width by $B_l = \exp\left(-l(l+1)\theta^2_{\rm fwhm}/2\ln 256\right)$ and $f_{\rm sky}$ is the sky fraction.

We will use the forthcoming Planck mission (The Planck Collaboration 2006) specifications for the measurements of the CMB temperature and polarization spectra. Note that Eq. (23) usually includes a summation over the Planck frequency channels. However we conservatively assume that we will only use the 143 GHz channel as science channel, with the other frequencies used for foreground removal (not treated in this paper). This channel has a beam of $\theta_{\rm fwhm} = 7.1'$ and sensitivities of $\sigma_T = 2.2\mu K/K$ and $\sigma_P = 4.2\mu K/K$. To account for the galactic plane cut, we take $f_{\rm sky} = 0.80$. Note we use as a minimum ℓ-mode, $\ell_{\rm min} = 30$ in order to avoid problems with polarization foregrounds and subtleties for the modeling of the integrated Sachs-Wolfe effect.

The Fisher matrix for TWL reads:

$$F^{\rm WL}_{\alpha\beta} = \qquad (30)$$
$$f_{sky}\sum_{\ell}^{\ell_{max}} \frac{(2\ell+1)\Delta\ell}{2}\frac{\partial P_{ij,\ell}}{\partial\theta_\alpha}P^{-1}_{jk,\ell}\frac{\partial P_{km,\ell}}{\partial\theta_\beta}P^{-1}_{mi,\ell}\ .$$

where $P_{ij,\ell}$ are the components of the non-linear weak lensing power spectrum for the i-th and j-th bin (Hu & Jain 2004). In the expression (30) a summation over repeated indices is implicit. The redshift bins have been chosen such that each contains the same amount of galaxies. We consider the 5 bin case as reference case.

The non-linear corrections are calculated using HALOFIT (Smith et al. 2003). This procedure is suitably fitted to ΛCDM N-body simulations. Therefore it could lead to errors of the order of 20% on Fisher outputs, if used for models different from ΛCDM (see *e.g.* Casarini et al. (2011)). However, in the absence of suitable extensions for MaVaN, we assume HALOFIT as the procedure for non-linear corrections, reporting results up to $\ell_{max} = 1000$, in the mildly non-linear regime. This conservative choice also prevent us from considering a regime in which baryons could strongly affect matter power spectra and, as a consequence, weak lensing spectra (Casarini et al. 2012).

The TWL survey parameters are fixed according to the forthcoming Euclid mission[1] specifications (Laureijs et al. 2011). The survey area covered by the experiment is 15000 deg^2, while the density is 30 galaxies per arcmin^2. The distribution of the galaxy number on the redshift and solid angle is $n(z) = n_0 z^2 e^{(z/z_0)^{1.5}}$ with a median redshift $\bar{z} = 0.9$. The photometric redshift error is $0.05\ (1+z)$.

The error estimation of DE and neutrino density parameters is reported for a MaVaN model with an exponential coupling for an increasing and decreasing neutrino mass. As shown in Tab. 2, TWL is able to put constraints stronger than CMB on β and ω_ν, with an improvement of ∼10% and >30%, respectively. On the contrary CMB is more efficient in constraining α, gaining ∼50% over TWL. The combination of the two observables can improve constraints on all parameters. In this case, the main result is for the estimate of ω_ν constraint to 0.00025, $\sigma_{m_\nu} \sim 0.02$eV. Analogous comments can be made for the $\beta > 0$ in Tab. 3, with the only difference that CMB can constrain β better than TWL.

[1] http://www.euclid-ec.org

TABLE 2
1-σ error estimations of cosmological parameters for an exponential potential with $\beta < 0$, using Planck-like CMB and Euclid-like Tomographic Weak Lensing (TWL) data with $\ell_{max} = 1000$, alone or in combination.

Dataset	σ_{ω_ν}	σ_α	σ_β
TWL	0.00043	0.024	1.17
CMB	0.00064	0.014	1.28
TWL+CMB	0.00025	0.012	0.69

TABLE 3
The same as Tab 2, but with $\beta > 0$.

Dataset	σ_{ω_ν}	σ_α	σ_β
TWL	0.00045	0.028	2.04
CMB	0.00054	0.019	1.71
TWL+CMB	0.00026	0.012	1.15

In Fig. 6, we show 1-σ and 2-σ likelihood contours for MaVan's model with an exponential coupling for both an increasing and decreasing neutrino mass. Here we report results for ω_ν, β and α, after marginalizing over the other parameters. It is quite clear that neither Planck nor Euclid alone will be able to constrain a non-zero coupling $\beta \sim \mathcal{O}(1)$, only TWL being slightly more efficient than CMB in the $\beta < 0$ case. In this case the combination of the two can exclude a null coupling with a significance higher than 2-σ.

Let us note that we performed a conservative analysis of TWL Fisher matrix, using multipoles up to $\ell_{max} = 1000$. The capability of TWL in constraining β and the other parameters will be significantly increased by the use of higher multipoles, delving into the deep non-linear regime. For instance Fig. 7 presents the confidence ellipses obtained including multipoles up to $\ell_{max} = 5000$ in the TWL Fisher matrix. Estimated errors are clearly reduced of a factor ∼2 with respect to Fig. 7 for Weak Lensing and, as a consequence, for the combined case. This figure shows that Euclid would be able to exclude the zero value both for β and ω_ν with high statistical significance. However in this case an appropriate extension of HALOFIT would be necessary, including both appropriate non-linear correction for MaVaN models and baryon physics.

Despite this limitation, a very interesting results is the fact that TWL, alone or in combination with CMB, is able to find a lower value to $\Omega_\nu h^2$ with an error half of the CMB error if taken alone. Moreover a strong degeneracy can be found in the ω_ν-β plane for what concerns the TWL ellipses, also if considered in combination with CMB. This effect appears in both cases in a symmetric way, showing that lower $|\beta|$ values allow higher neutrino mass. The $\Omega_\nu h^2$-β degeneracy could be eventually bro-

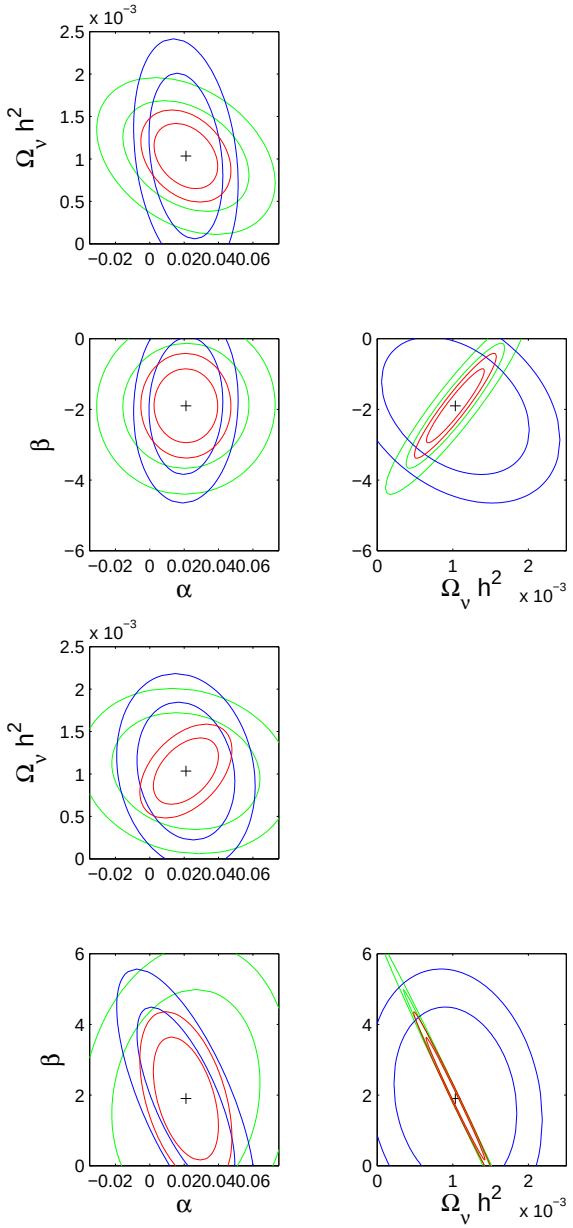

FIG. 6.— Upper (lower) panel shows likelihood contour forecast at 68% and 95% confidence levels for the exponential potential, in the decreasing (increasing) mass case. We marginalized over the other parameters. The green lines are obtained considering a tomographic weak lensing Euclid-like survey, with 5 bins and $\ell_{max} = 1000$. The blue lines are for a Planck-like CMB mission. The red lines are for a combination of the two. The crosses indicate the fiducial values

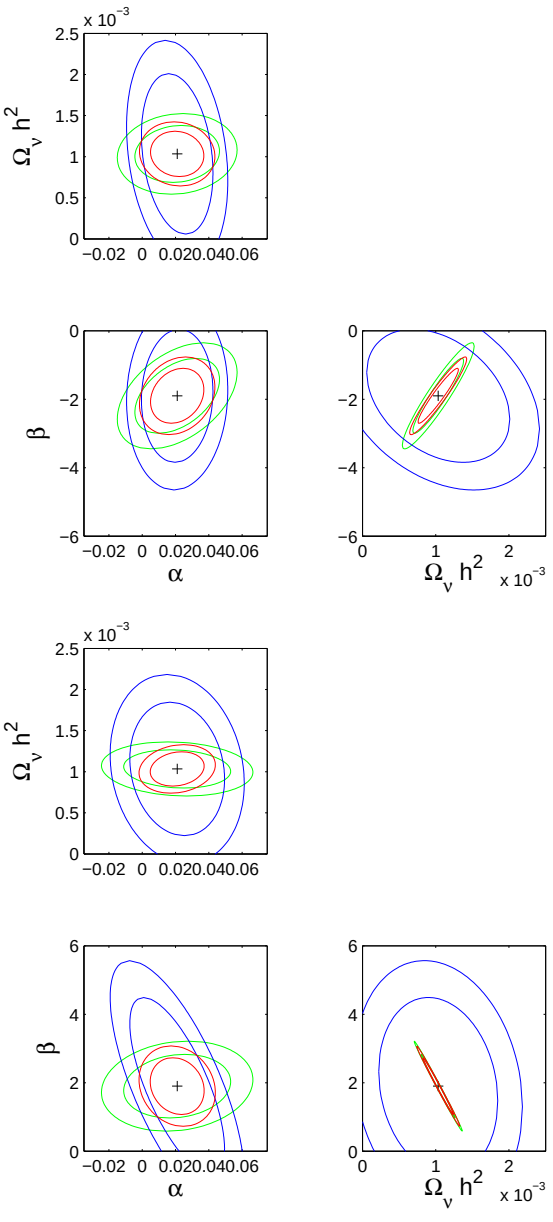

FIG. 7.— As Fig 6 with 5 bins and $\ell_{max} = 5000$.

ken from external priors on m_ν. On the other hand, no noteworthy remark can be said about the α parameter, whose constrains remains compatible with zero also for the combination of the two observables.

6. DISCUSSION AND CONCLUSIONS

In this work we focused on the hypothesis that the origin of the cosmic acceleration can be attributed to a quintessence scalar field coupled to massive neutrinos. Firstly, we updated and extended parameter constraints using the most recent available data from SNIa, CMB and LSS observations. We considered both an exponential and a power law potential, with increasing ($\beta > 0$) or decreasing ($\beta < 0$) neutrino mass.

In none of these cases the cosmological data placed strong constraints on the coupling parameter in the low coupling range. Neither for the neutrino density parameter, on which only upper limits can be placed. The main outcome of the analysis was that β values $\sim \mathcal{O}(1)$ are compatible with actual data, together with a neutrino mass $m_\nu \lesssim 0.32$eV.

Therefore at the moment we do have not enough information to exclude a possible coupling between neutrino and DE field, neither in the low or in the high coupling regime. New and precise data from observables related to the recent evolution of the universe are necessary together with a deeper understanding of the MaVaN theory dynamics. In this sense the forthcoming Euclid weak lensing and galaxy clustering data will represent

the turning point for the future progress in cosmology.

With this aim, a Fisher matrix study was accomplished, considering future data release from missions such as Planck for CMB spectra and Euclid for tomographic weak lensing spectra. The latter experiment will be more efficient in improving present constraints on ω_ν, even considering a cautious use of multipoles up to $\ell_{max} = 1000$. This choice prevent us from including highly non-linear features, which are not correctly predicted by HALOFIT for MaVaN theories. Combining Euclid data with complementary information from Planck will exclude a zero coupling at more than 2-σ. It is worth to mention the strong degeneracy between β and ω_ν, which could eventually be broken by an external prior on the neutrino mass.

A crucial point for the forthcoming Euclid mission will be the study and implementation of an efficient way of including non-linear corrections on the matter power spectrum calculations, HALOFIT being only suitable for ΛCDM cosmologies. In fact, delving into the deep non-linear regime of matter perturbations could significantly improve parameter estimation, fully exploiting the high potentiality of the TWL from Euclid.

ACKNOWLEDGMENTS

GLV and DFM thank Valeria Pettorino for useful comments and discussions.DFM thanks the Research Council of Norway FRINAT grant 197251/V30. DFM is also partially supported by project CERN/FP/123615/2011 and PTDC/FIS/111725/2009.

REFERENCES

Afshordi, N., Zaldarriaga, M., & Kohri, K. 2005, Phys.Rev., D72, 065024
Amanullah, R., Lidman, C., Rubin, D., Aldering, G., Astier, P., et al. 2010, Astrophys.J., 716, 712
Amendola, L. 2000, Phys.Rev., D62, 043511
Amendola, L., Baldi, M., & Wetterich, C. 2008a, Phys.Rev., D78, 023015
—. 2008b, Phys.Rev., D78, 023015
Amendola, L., Pettorino, V., Quercellini, C., & Vollmer, A. 2011, arXiv:1111.1404 [astro-ph.CO]
Ayaita, Y., Weber, M., & Wetterich, C. 2011, arXiv:1112.4762 [astro-ph.CO]
Baldi, M. 2011, arXiv:1110.2173 [astro-ph.CO]
Baldi, M., Pettorino, V., Amendola, L., & Wetterich, C. 2011a, arXiv:1106.2161 [astro-ph.CO]
—. 2011b
Bernardini, A., & Bertolami, O. 2008, J.Phys.Conf.Ser., 136, 042066
Bernardini, A. E., & Bertolami, O. 2009, PoS, ISFTG, 024
Bi, X.-J., Feng, B., Li, H., & Zhang, X.-m. 2005, Phys.Rev., D72, 123523
Binetruy, P. 1999, Phys.Rev., D60, 063502
Bjaelde, O. E., Brookfield, A. W., van de Bruck, C., Hannestad, S., Mota, D. F., et al. 2008, JCAP, 0801, 026
Brookfield, A., van de Bruck, C., Mota, D., & Tocchini-Valentini, D. 2006a, Phys.Rev.Lett., 96, 061301
Brookfield, A. W., van de Bruck, C., Mota, D., & Tocchini-Valentini, D. 2006b, Phys.Rev., D73, 083515
Brouzakis, N., Pettorino, V., Tetradis, N., & Wetterich, C. 2011, JCAP, 1103, 049
Casarini, L., Bonometto, S. A., Borgani, S., Dolag, K., Murante, G., et al. 2012, arXiv:1203.5251 [astro-ph.CO]
Casarini, L., La Vacca, G., Amendola, L., Bonometto, S. A., & Maccio, A. V. 2011, JCAP, 1103, 026
de Holanda, P. C. 2009, JCAP, 0907, 024
Dickinson, C., Battye, R. A., Carreira, P., Cleary, K., Davies, R. D., et al. 2004, Mon.Not.Roy.Astron.Soc., 353, 732
Fardon, R. 2008, aAT-0820478
Fardon, R., Nelson, A. E., & Weiner, N. 2004, JCAP, 0410, 005
Ferreira, P. G., & Joyce, M. 1998, Phys.Rev., D58, 023503
Fisher, R. A. 1935, J. Roy. Statist. Soc., 98, 39
Franca, U., Lattanzi, M., Lesgourgues, J., & Pastor, S. 2009, Phys.Rev., D80, 083506
Honda, M., Takahashi, R., & Tanimoto, M. 2006, JHEP, 0601, 042
Hu, W., & Jain, B. 2004, Phys.Rev., D70, 043009
Keum, Y.-Y. 2007, Mod.Phys.Lett., A22, 2131
Klapdor-Kleingrothaus, H., Krivosheina, I., Dietz, A., & Chkvorets, O. 2004, Phys.Lett., B586, 198
Klapdor-Kleingrothaus, H. V. 2005, 215, hep-ph/0512263
Komatsu, E., et al. 2011, Astrophys.J.Suppl., 192, 18
Kowalski, M., et al. 2008, Astrophys.J., 686, 749
Kristiansen, J., La Vacca, G., Colombo, L., Mainini, R., & Bonometto, S. 2010, New Astron., 15, 609
La Vacca, G., Kristiansen, J. R., Colombo, L. P. L., Mainini, R., & Bonometto, S. A. 2009, JCAP, 0904, 007
Laureijs, R., Amiaux, J., Arduini, S., Augueres, J.-L., Brinchmann, J., et al. 2011, arXiv:1110.3193 [astro-ph.CO]
Lewis, A., & Bridle, S. 2002, Phys. Rev., D66, 103511
Lewis, A., Challinor, A., & Lasenby, A. 2000, Astrophys.J., 538, 473
Masiero, A. 2005, 131, prepared for 11th International Workshop on Neutrino Telescopes
Mota, D., Pettorino, V., Robbers, G., & Wetterich, C. 2008, Phys.Lett., B663, 160
Nunes, N. J., Schrempp, L., & Wetterich, C. 2011, Phys.Rev., D83, 083523
Peebles, P. J. E., & Ratra, B. 1988, ApJ, 325, L17
Perlmutter, S., et al. 1999, Astrophys.J., 517, 565
Pettorino, V. 2009, Nucl.Phys.Proc.Suppl., 194, 300
Pettorino, V., Mota, D. F., Robbers, G., & Wetterich, C. 2009, AIP Conf.Proc., 1115, 291
Pettorino, V., Wintergerst, N., Amendola, L., & Wetterich, C. 2010, Phys.Rev., D82, 123001
Rassat, A., Amara, A., Amendola, L., Castander, F. J., Kitching, T., et al. 2008, arXiv:0810.0003 [astro-ph]
Reichardt, C., Ade, P., Bock, J., Bond, J., Brevik, J., et al. 2009, Astrophys.J., 694, 1200
Reid, B. A., Percival, W. J., Eisenstein, D. J., Verde, L., Spergel, D. N., et al. 2010, Mon.Not.Roy.Astron.Soc., 404, 60
Riess, A. G., Macri, L., Casertano, S., Sosey, M., Lampeitl, H., et al. 2009, Astrophys.J., 699, 539
Riess, A. G., et al. 1998, Astron.J., 116, 1009
Sievers, J. L., Achermann, C., Bond, J., Bronfman, L., Bustos, R., et al. 2007, Astrophys.J., 660, 976
Smith, R., et al. 2003, Mon.Not.Roy.Astron.Soc., 341, 1311
Spitzer, C. 2006, astro-ph/0606034
Steinhardt, P. J., Wang, L.-M., & Zlatev, I. 1999, Phys.Rev., D59, 123504
Sturm, M. 2011, arXiv:1111.4773 [hep-ex]
Sullivan, M., Guy, J., Conley, A., Regnault, N., Astier, P., et al. 2011, Astrophys.J., 737, 102
Tegmark, M., Taylor, A., & Heavens, A. 1997, Astrophys.J., 480, 22
Tegmark, M., et al. 2006, Phys.Rev., D74, 123507
The Planck Collaboration. 2006, arXiv:astro-ph/0604069
Wetterich, C. 1988, Nuclear Physics B, 302, 645
—. 1995, Astron.Astrophys., 301, 321
—. 2007, Phys.Lett., B655, 201
Wetterich, C., & Pettorino, V. 2009, 561, arXiv:0905.0715 [astro-ph.CO]
Wintergerst, N., Pettorino, V., Mota, D., & Wetterich, C. 2010, Phys.Rev., D81, 063525
Wood-Vasey, W. M., et al. 2007, Astrophys.J., 666, 694
Zaldarriaga, M., & Seljak, U. 1997, Phys.Rev., D55, 1830
Zaldarriaga, M., Spergel, D. N., & Seljak, U. 1997, Astrophys.J., 488, 1